

MECHANISMS  
OF CATALYTIC REACTIONS

# Formation of Co–Ru/MgO/Al<sub>2</sub>O<sub>3</sub> Catalysts for the Fischer–Tropsch Synthesis: A Magnetic Method for the Estimation of Cobalt Particle Size

G. V. Pankina<sup>a</sup>, P. A. Chernavskii<sup>a</sup>, A. Yu. Krylova<sup>b</sup>, and V. V. Lunin<sup>a</sup>

<sup>a</sup> Department of Chemistry, Moscow State University, Moscow, 119992 Russia

<sup>b</sup> Joint Research and Development Center, Moscow, Russia

e-mail: pankina@kge.msu.ru

Received June 22, 2006

**Abstract**—The physicochemical properties of Co-supported catalysts were studied, and the particle size of Co in Co/MgO/Al<sub>2</sub>O<sub>3</sub> and Co–0.2% Ru/MgO/Al<sub>2</sub>O<sub>3</sub> catalysts for the Fischer–Tropsch synthesis (FTS) was estimated using a magnetic method. It was found that a considerable fraction of superparamagnetic Co particles, which increase selectivity for C<sub>5+</sub> hydrocarbons and decrease the yield of methane in the FTS, was present in a ruthenium-containing catalyst along with single-domain ferromagnetic particles. In this case, the catalyst activity increased by a factor of 10.

**DOI:** 10.1134/S0023158407040143

## INTRODUCTION

It is well known that the particle size of cobalt metal in Co-supported catalysts for the Fischer–Tropsch synthesis (FTS) is mainly responsible for the activity and selectivity of the process [1, 2]. In these catalysts, cobalt is frequently in the superparamagnetic state because of the small particle size (of about several nanometers). The presence of small cobalt particles facilitates an increase in the selectivity for methane. However, the selectivity for heavy hydrocarbons in the FTS increases with particle size, although the overall activity decreases in this case because of a decrease in the specific surface area of the metal. Thus, it is likely that there is an optimum size of Co particles in Co-supported FTS catalysts at which a reasonable selectivity for C<sub>5+</sub> and a high activity are reached.

The particle size of supported cobalt depends on the pore size of the support (it increases with pore diameter [1]), as well as a number of other factors, in particular, the presence of promoters for cobalt reduction from an oxide [3]. Saib et al. [4] found that 20% Co/SiO<sub>2</sub> with a pore diameter of 10 nm exhibited high activity and selectivity for hydrocarbons. Note that the pore structure of a support had also a considerable effect on FTS selectivity [5]. Therefore, supports with identical pore structures should be used in order to reveal the effect of Co particle size on selectivity.

Supports with small pore diameters, such as mesoporous silica gel or γ-Al<sub>2</sub>O<sub>3</sub>, are commonly used for the synthesis of a catalyst containing superparamagnetic cobalt particles (for Co at T = 20°C, these particles are smaller than 7–8 nm). In this case, the promotion of the active catalyst component with noble metals (Ru or Re

[1, 6, 7]) provides an opportunity to affect the dispersion of cobalt.

In this work, we considered the effect of a promoting additive of Ru on the particle size of Co, as well as the effect of the average particle size of Co on the selectivity and activity of Co/MgO/Al<sub>2</sub>O<sub>3</sub> and Co–Ru/MgO/Al<sub>2</sub>O<sub>3</sub> catalysts in the FTS.

## EXPERIMENTAL

The 0.5% MgO/Al<sub>2</sub>O<sub>3</sub> support was prepared by the impregnation of γ-Al<sub>2</sub>O<sub>3</sub> (A-64; S<sub>sp</sub> = 220 m<sup>2</sup>/g; V<sub>pore</sub> = 0.75 cm<sup>3</sup>/g) with a solution of Mg(NO<sub>3</sub>)<sub>2</sub> · 6H<sub>2</sub>O followed by drying at 90°C and calcination at 500°C for 6 h in order to form the spinel structure MgAl<sub>2</sub>O<sub>3+x</sub>, where x ≤ 1, in the surface layer of γ-Al<sub>2</sub>O<sub>3</sub>. The catalysts Co/0.5% MgO/Al<sub>2</sub>O<sub>3</sub> (**I**) and Co–0.2% Ru/0.5% MgO/Al<sub>2</sub>O<sub>3</sub> (**II**) were prepared by successive impregnation with a solution of Co(NO<sub>3</sub>)<sub>2</sub> · 6H<sub>2</sub>O or a mixture of solutions of Co(NO<sub>3</sub>)<sub>2</sub> · 6H<sub>2</sub>O and RuCl<sub>3</sub> · nH<sub>2</sub>O with required concentrations, respectively. After each stage of impregnation (the supporting of 10, 20, and 30 wt % Co, respectively), the catalysts were dried and calcined in a flow of air at 450°C for 2 h. Two series of catalysts containing 10, 20, and 30 wt % Co were prepared in this manner.

A flow microreactor served as the measuring cell of a vibration magnetometer; this allowed us to perform the in situ measurements of magnetization in the course of the reaction. The test sample was fixed between two porous quartz membranes. A katharometer was used as a detector at the reactor outlet. The magnetometer was calibrated using a sample of high-purity cobalt before

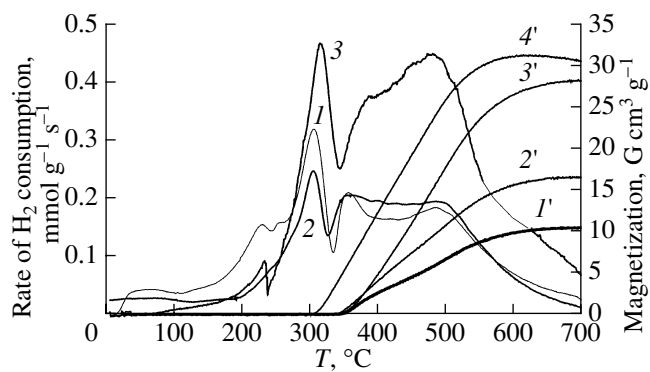


**Fig. 1.** (1–3) TPR spectra and (1'–3') the temperature dependence of magnetization for the Co/0.5% MgO/Al<sub>2</sub>O<sub>3</sub> catalyst with Co content of (1) 10, (2) 20, or (3) 30 wt %; (4') changes in the magnetization of a sample with 30% Co in the course of TPR in an atmosphere of pure H<sub>2</sub>.

each particular experiment. Magnetization was assumed proportional to the weight of cobalt metal. The heating rate was 0.5 K/s in all of the nonisothermal experiments. The weight of a catalyst sample was constant and equal to 20 mg.

Temperature-programmed reduction (TPR) was carried out in a flowing mixture of 5 vol % H<sub>2</sub> + Ar. Reduction was monitored as the hydrogen uptake rate and as the variation of magnetization.

Immediately before temperature-programmed oxidation, the catalyst was reduced in hydrogen at 700°C to constant magnetization, which corresponded to the degree of cobalt reduction of ~70–80%. After the reduction, the catalysts were cooled to 7°C in a flow of high-purity argon.

Oxidation was performed under isothermal conditions at 7°C in a mixture of 1 vol % O<sub>2</sub> + He. In this case, an oxide film, which was stable at the specified temperature, was formed and further oxidation was possible only with increasing temperature.

The coercive force  $H_c$  and residual magnetization were measured at 7°C. The saturation magnetization  $\sigma_s$  was determined by extrapolating to infinite field in the 1/H–σ coordinates.

The particle size of cobalt was estimated after reduction in a flow of H<sub>2</sub> at 700°C. The degree of reduction was monitored by measuring magnetization changes. Upon reaching a constant magnetization, the test sample was cooled to 200°C and the flow of hydrogen was replaced with argon in order to desorb H<sub>2</sub> from the surface of cobalt. Then, the temperature was decreased to the temperature of water in the microfurnace cooler (7°C). The field dependence of the magnetization of samples at room temperature was measured on a vibration magnetometer with a maximum field of 6.3 kOe.

The catalytic tests of samples were performed in a GTL/HP 4 catalytic setup using a mixture of CO + H<sub>2</sub> +

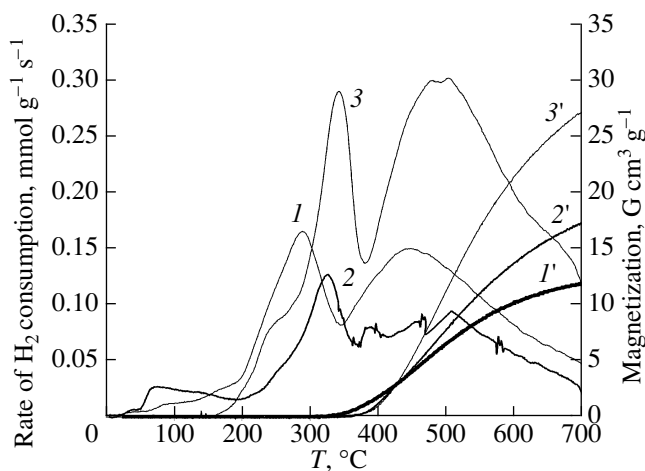


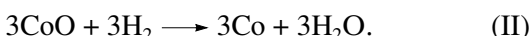
**Fig. 2.** (1–3) TPR spectra and (1'–3') the temperature dependence of magnetization for the Co–0.2% Ru/0.5% MgO/Al<sub>2</sub>O<sub>3</sub> catalyst with Co content of (1) 10, (2) 20, or (3) 30 wt %.

5% N<sub>2</sub> at a reactor pressure of 20 atm. The catalyst volume was 5 cm<sup>3</sup>. The working temperature was varied from 170 to 205°C. The space velocity of synthesis gas was 1000 h<sup>-1</sup>. The reaction products were analyzed by chromatography. The gas mixtures of CO, N<sub>2</sub>, and H<sub>2</sub> were separated on a column packed with molecular sieves CaA; CH<sub>4</sub>, C<sub>2</sub>–C<sub>4</sub>, and CO<sub>2</sub> were separated on a column with a HayeSep phase, and C<sub>5+</sub> hydrocarbons were separated on a DP-Petro 0.5 capillary column (50 m × 0.2 mm).

## RESULTS AND DISCUSSION

### Temperature-Programmed Reduction

Figures 1 and 2 show the temperature-programmed reduction (TPR) spectra and the temperature dependence of magnetization for catalysts I and II, respectively. Previously, it was found that the formation of the spinel structure MgAl<sub>2</sub>O<sub>3+x</sub> in the surface layer of γ-Al<sub>2</sub>O<sub>3</sub> prevents the oxide–oxide interaction of the active component with the support to result in a more complete reduction [8]. The reduction process is a two-step reaction of Co<sub>3</sub>O<sub>4</sub> reduction to cobalt metal. It is well known that two peaks in the TPR spectra correspond to the processes [10]



Only the reduction process CoO → Co is accompanied by an increase in magnetization to a constant value that corresponds to the degree of reduction. This value was ~80% for our catalysts. In this case, the completion of reduction can also be judged from an insignificant decrease in magnetization at the end of the process because of the temperature dependence of magnetization.

In Figs. 1 and 2, it can be seen that the temperature of the appearance of cobalt metal in the presence of the ruthenium promoter increased from 330 to 360°C with increasing cobalt concentration. In the absence of ruthenium, this temperature was almost independent of the cobalt concentration and equal to ~340°C. Nevertheless, note that the rate of reduction of catalyst **I** was higher than that of catalyst **II**. However, as judged from the final magnetization, the degrees of reduction were equal in both of the catalysts. As can be seen in Fig. 1, the degree of reduction of 30% Co/0.5% MgO/Al<sub>2</sub>O<sub>3</sub> was much higher if the catalyst was reduced in an atmosphere of pure hydrogen. It is likely that, in this case, the expected promoting effect of ruthenium, which is related to the spillover of hydrogen on the support surface or a CoO<sub>x</sub> phase, is weakened by the fact that ruthenium particles are arranged in the narrow pores of the support and the spillover of hydrogen is suppressed [11].

#### Dependence of Magnetization on Magnetic Field Intensity and Cobalt Particle Size

The particle size of cobalt was estimated from the dependence of magnetization on magnetic field intensity for catalysts **I** and **II** at room temperature by measuring coercive force ( $H_c$ ) before and after the partial oxidation of cobalt nanoparticles.

Figure 3 shows the dependence of magnetization on magnetic field intensity for the 30% Co/0.5% MgO/Al<sub>2</sub>O<sub>3</sub> catalyst. The occurrence of a hysteresis in the curve suggests that nonsuperparamagnetic cobalt particles were present in the system. The 10% Co and 30% Co/0.5% MgO/Al<sub>2</sub>O<sub>3</sub> catalysts also exhibited a hysteresis.

To answer the question of which particular type of particles was predominant in the test systems, we used the following methodology: It is well known [12] that the dependence of the coercive force on the particle size of a ferromagnetic has the shape of a curve with a maximum. For cobalt, a maximum of  $H_c$  corresponds to a size of ~20 nm (single-domain particles) [13]. A dramatic decrease in  $H_c$  was observed as the particle size decreased from 20 nm. In the transition to a superparamagnetic state,  $H_c$  became zero. For particles whose size was greater than ~20 nm (multidomain particles),  $H_c$  also decreased but to a limit that corresponded to bulk metal. On the other hand, a decrease in the size of a particle metal core because of oxide film formation was observed in low-temperature oxidation ( $T_{ox} < 330^\circ\text{C}$ ). In accordance with the above, the oxidation of cobalt particles results in coercive force changes towards increasing  $H_c$  in the case that the system contains particles of size greater than ~20 nm or towards decreasing  $H_c$  if the system consists of particles smaller than ~20 nm. If the system does not contain multidomain particles, that is,  $d < 20$  nm, the following equation can be used to analyze the particle-size distribution [14]:

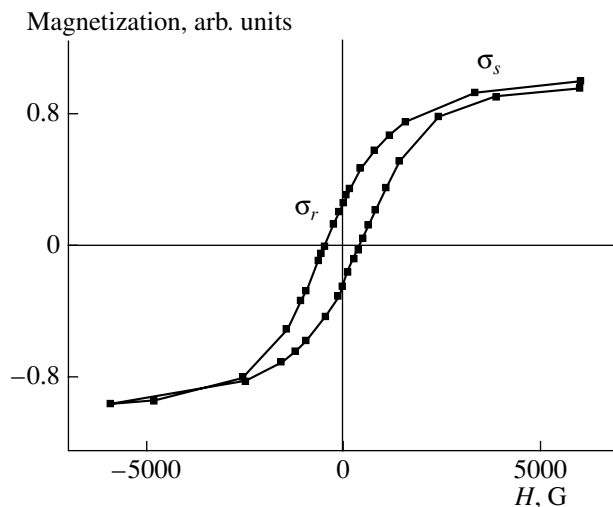


Fig. 3. Dependence of magnetization on magnetic field intensity ( $H$ ) for the 30 wt % Co/0.5% MgO/Al<sub>2</sub>O<sub>3</sub> catalyst.

$$\gamma = 1 - 2\sigma_r/\sigma_s, \quad (1)$$

where  $\gamma$  is the fraction of superparamagnetic particles,  $\sigma_r$  is the residual magnetization, and  $\sigma_s$  is the saturation magnetization.

The upper limit of the size of superparamagnetic particles at room temperature can be estimated using the equation

$$KV = 30kT, \quad (2)$$

where  $K$  is the anisotropy constant of fcc Co, which is equal to  $5 \times 10^6$  erg/cm<sup>3</sup> [15], and  $V$  is the particle volume. The greatest diameter of superparamagnetic particles that satisfies Eq. (2) at  $T = 7^\circ\text{C}$  (the measurement temperature) is ~7.6 nm.

Table 1 summarizes characteristics of catalysts **I** and **II**. It can be seen that an increase in  $H_c$  in the partial oxidation of catalyst **I** at all Co concentrations suggests the presence of multidomain cobalt particles in this catalyst. As for catalyst **II**, the value of  $H_c$  passed through a maximum as the concentration of cobalt was increased. In this case, an insignificant increase in  $H_c$  was observed in the partial oxidation of a catalyst with 10% Co, as compared with that of the reduced sample, whereas  $H_c$  decreased in the samples with 20 and 30% Co. Thus, catalysts **II** with Co concentrations of 20 and 30 wt % did not contain multidomain particles; consequently, the particle size of cobalt in these catalysts was smaller than 20 nm. For these catalysts, Eq. (1) can be used in order to evaluate the fraction of particles of sizes from 20 to 7.6 nm and particles smaller than 7.6 nm, that is, superparamagnetic cobalt particles. The corresponding data are given in Table 1.

We calculated that, in catalyst **II** with a cobalt content of 30%, the fraction of particles of size from 7.6 to 20 nm was 46% and the fraction of superparamagnetic particles was 54%. This is consistent with conclusions

**Table 1.** Properties of Co/0.5% MgO/Al<sub>2</sub>O<sub>3</sub> (**I**) and Co–0.02% Ru/0.5% MgO/Al<sub>2</sub>O<sub>3</sub> (**II**) catalysts

Cobalt content, %	<i>H</i> <sub>c</sub> , Oe		TPR data			Amount of Co particles, %	
	after TPR	after TPO	<i>T</i> <sub>Co formation</sub> , °C	<i>T</i> <sub>peak I</sub> , °C	<i>T</i> <sub>peak II</sub> , °C	7.6 nm < <i>d</i> < 20 nm (nonsuperparamagnetic)	<i>d</i> ≤ 7.6 nm (superparamagnetic)
<b>Catalyst I</b>							
10	363	390	340	300	350–480	–	–
20	453	525	340	300	240–500	–	–
30	476	–	340	310	480	–	–
<b>Catalyst II</b>							
10	286	320	310	280	420	–	–
20	430	400	340	300	350–490	50	50
30	295	176	360	330	490	46	54

**Table 2.** Catalytic tests of samples **I** and **II**

<i>t</i> , h	<i>T</i> , °C	<i>X</i> <sub>CO</sub> , %	Yield, g/m <sup>3</sup>					<i>S</i> <sub>C<sub>5+</sub></sub> , %	<i>S</i> <sub>CH<sub>4</sub></sub> , %	<i>A</i> × 10 <sup>6</sup> , mol CO (g Co) <sup>-1</sup> s <sup>-1</sup>	Composition of liquid hydrocarbons, %			Composition of paraffins, %			<i>α</i>	<i>n</i> -/iso, %/%
			CH <sub>4</sub>	C <sub>2</sub> –C <sub>4</sub>	C <sub>5+</sub>	CO <sub>2</sub>	Σ <sub>HC</sub>				olefins	<i>n</i> -paraffins	isoparaffins	C <sub>5</sub> –C <sub>10</sub>	C <sub>11</sub> –C <sub>18</sub>	C <sub>19</sub>		
30% Co–Ru/0.5% MgO/Al <sub>2</sub> O <sub>3</sub> ( <b>II</b> )																		
7	170	1.3	0.5	0.5	1.6	0.4	2.6	60.1	17.5	0.26	–	–	–	–	–	–	–	
14	180	3.9	1.6	2.0	4.3	0.6	7.9	55.0	18.2	0.80	–	–	–	–	–	–	–	
21	190	16.8	4.8	5.5	24.2	1.2	34.5	71.2	12.2	3.44	–	–	–	–	–	–	–	
28	200	49.7	10.3	7.3	83.4	3.1	101.0	83.0	9.0	9.86	10.5	73.2	16.3	47.2	49.1	3.8	0.81	4.5
30% Co/0.5% MgO/Al <sub>2</sub> O <sub>3</sub> ( <b>I</b> )																		
7	170	1.6	0.1	0	3.1	0.2	3.2	94	4.0	0.21	–	–	–	–	–	–	–	
14	180	3.4	0.4	0.8	5.7	0.4	6.9	83	4.5	0.45	–	–	–	–	–	–	–	
21	190	3.8	1.0	1.0	5.8	0.6	7.8	74	11.7	0.51	–	–	–	–	–	–	–	
28	200	7.9	2.4	2.0	12.0	1.0	14.4	73	13.0	1.02	–	–	–	–	–	–	–	
35	210	17.0	5.1	2.0	26.5	1.0	33.6	76	12.7	2.22	1.4	89.6	9.0	28.5	58.9	12.6	0.93	10.0
42	215	28.8	7.9	6.2	45.5	2.4	59.6	77.0	11.6	3.78	2.2	89.9	7.8	17.9	67.6	14.5	0.92	11.5
49	220	42.6	19.7	3.6	65.3	4.9	88.6	74.7	19.7	5.64	–	–	–	–	–	–	–	
56	225	51.2	37.9	10.5	58.1	11.9	106.5	55.3	31.6	6.73	1.2	89.1	9.6	40.3	48.7	11.0	0.84	9.3
63	230	65.3	51.9	15.7	65.1	27.0	132.7	48.6	33.9	8.64	–	–	–	–	–	–	–	

Notes: Reduction conditions: H<sub>2</sub>, 400°C; 4 h; 1000 h<sup>-1</sup>. FTS conditions: CO + H<sub>2</sub> + 5% N<sub>2</sub>; *P* = 20 atm.

Notation: *X* is conversion; *S* is selectivity; *A* is activity; Σ<sub>HC</sub> is the Schulz–Flory coefficient.

drawn based on the oxidation of these catalysts. The corresponding values for catalysts after the first and second impregnations (Co concentrations of 10 and 20%, respectively) were 61 and 50%, respectively. As noted above, catalyst **I** contained multidomain Co particles (greater than 20 nm); in this case, it is incorrect to judge the particle-size distribution from magnetic measurements.

In this context, the positions of peaks in the TPR spectra of catalysts **I** and **II** became understandable. Indeed, in the case of a catalyst containing 30 wt % Co, the maximum temperatures of the first and second peaks of catalyst **II** were higher than those of catalyst **I**. This was due to the presence of superparamagnetic Co particles because the reducibility decreases with decreasing particle size [16]. It is well known that the

equilibrium temperature of reduction to metal increases with decreasing metal oxide particle size [16]. For catalyst **I**, the peak maximum temperatures remained almost unchanged from impregnation to impregnation because the particle size of cobalt did not decrease.

### Catalytic Tests

Table 2 summarizes the results of the catalytic tests of catalysts **I** and **II**. It can be seen that a CO conversion of almost 50% and 9 and 83% selectivity for CH<sub>4</sub> and C<sub>5+</sub>, respectively, were reached on catalyst **II** even after 28-h operation at 200°C. At the same time, on catalyst **I** under the specified conditions, the conversion of CO was 7.9% and the selectivity for methane and C<sub>5+</sub> was 13 and 73%, respectively. The further operation of this catalyst (225°C; 56 h) resulted in an increase in conversion to 51.2% and in selectivity for methane to 32% and in a decrease in selectivity for C<sub>5+</sub> hydrocarbons. The yield of olefins was insignificant (1.2%), whereas it was higher by an order of magnitude on a catalyst with ruthenium at a shorter operation time (28 h). As for the Schulz–Flory coefficient ( $\alpha$ ), it is as high as 0.93 for catalyst **I** because of the considerably higher concentration of C<sub>11</sub>–C<sub>19</sub> paraffins in the products. Thus, the presence of ruthenium resulted in a noticeable change in the composition of synthetic products. In our opinion, the reason for this change in the composition is a decrease in the average particle size of Co particles upon the reduction of the catalyst in the presence of Ru.

Evidently, the much higher conversion of CO on catalyst **II** was due to the fact that the specific surface area of cobalt metal was higher than that in catalyst **I** because the average particle size of cobalt in catalyst **II** was smaller at the same degree of reduction and concentration of cobalt.

Thus, the presence of superparamagnetic and single-domain cobalt particles in Co-supported catalysts resulted in an increase in selectivity for C<sub>5+</sub> hydrocarbons and in low selectivity for methane, whereas these characteristics were much lower in a catalyst that consisted of larger (more than 20 nm) cobalt particles.

### ACKNOWLEDGMENTS

We are grateful to S.A. Sviderskii for his assistance in performing the catalytic tests.

This work was supported by the Russian Foundation for Basic Research (project no. 06-03-32500).

### REFERENCES

- Khodakov, A.Y., Grihval-Constant, A., Behara, R., and Zholobenko, V.L., *J. Catal.*, 2002, vol. 206, p. 230.
- Lapidus, A. and Krylova, A., *Appl. Catal.*, 1992, vol. 80, p. 1.
- Chernavskii, P.A., Khodakov, A.Y., Pankina, G.V., Girardon, J.-S., and Quinet, E., *Appl. Catal.*, 2006, vol. 306, p. 108.
- Saib, A.M., Claeys, M., and van Steen, E., *Catal. Today*, 2002, vol. 71, p. 395.
- Iglesia, E., *Appl. Catal.*, 1997, vol. 161, p. 59.
- Chernavskii, P.A., *Kinet. Katal.*, 2005, vol. 45, no. 5, p. 674 [*Kinet. Catal.* (Engl. Transl.), vol. 45, no. 5, p. 634].
- Chernavskii, P.A., Pankina, G.V., and Lermontov, A.S., *Zh. Fiz. Khim.*, 2005, vol. 79, no. 6, p. 1014 [*Rus. J. Phys. Chem.* (Engl. Transl.), vol. 79, no. 6, p. 875].
- Pankina, G.V., Chernavskii, P.A., and Lunin, V.V., *Kinet. Katal.*, 2005, vol. 46, no. 5, p. 764 [*Kinet. Catal.* (Engl. Transl.), vol. 46, no. 5, p. 719].
- Chernavskii, P.A., Pankina, G.V., and Lunin, V.V., *Catal. Lett.*, 2000, vol. 66, p. 121.
- Van de Loosdrecht, J., van der Haar, M., van der Kraan, A.M., van Dillen, A.J., and Geus, J.W., *Appl. Catal.*, 1997, vol. 150, p. 365.
- Saib, A.M., Borgna, A., van de Loosdrecht, J., van Berge, P.J., Geus, J.W., and Niemantsverdriet, J.W., *J. Catal.*, 2006, vol. 239, p. 326.
- Petrov, Yu.I., *Fizika malykh chastits* (Physics of Small Particles), Moscow: Nauka, 1982.
- Sort, J., Surinach, S., Munoz, J.S., Baro, M.D., et al., *Phys. Rev. B: Condens. Matter*, 2003, vol. 68, p. 014421.
- Barbier, A., Tuel, A., Arcon, I., Kodre, A., and Martin, G.A., *J. Catal.*, 2001, vol. 200, p. 106.
- Chen, J.P., Sorensen, C.M., and Klabunde, K.J., *Phys. Rev. B: Condens. Matter*, 1995, vol. 51, p. 11527.
- Huijuan Bi, Weiping Cai, and Caixia Kan, *J. Appl. Phys.*, 2002, vol. 92, p. 7491.